Icarus 237 (2014) 340–349

Contents lists available at ScienceDirect

Icarus

journal homepage: www.elsevier.com/locate/icarus

Observations of CO dayglow at 4.7 μm, CO mixing ratios, and temperatures at 74 and 104–111 km on Venus

Vladimir A. Krasnopolsky *,[1]

Department of Physics, Catholic University of America, Washington, DC 20064, USA
Moscow Institute of Physics and Technology, Dolgoprudny 141700, Russia

ARTICLE INFO

Article history:
Received 24 December 2013
Revised 24 April 2014
Accepted 24 April 2014
Available online 10 May 2014

Keywords:
Abundances, atmospheres
Atmospheres, composition
Venus
Venus, atmosphere
Infrared observations

ABSTRACT

The CO dayglow at 4.7 μm on Venus has been observed using the long-slit high-resolution spectrograph CSHELL at NASA IRTF with a resolving power of 4×10^4. The observations covered a latitude range of ±60° at local time of 07:50 at low latitudes. Solar lines in the spectra are used to measure Venus reflectivity which is found to be of 0.077 at 4.7 μm. Intensity ratio of the P2, P1, and R1 lines of the CO dayglow at the fundamental band (1-0) differs from that calculated by Crovisier et al. (Crovisier, J., Lellouch, E., de Bergh, C., Maillard, J.P., Lutz, B.L., Bezard, B. [2006]. Planet. Space Sci. 54, 1398–1414) and is closer to that expected at local thermodynamic equilibrium. The CO (1-0) dayglow is optically thick, its intensity weakly depends on the CO abundance and it proves poorly accessible for diagnostics of the Venus atmosphere. Six observed lines of the CO dayglow at the hot (2-1) band show a significant limb brightening typical of an optically thin airglow. Vertical intensities of the CO (2-1) band corrected for viewing angle and the Venus reflection are constant at 3.3 MR in the latitude range of ±50° at a solar zenith angle of 64°. Rotational temperatures of the CO (2-1) dayglow should reflect ambient temperature near 111 km. The observed temperatures are slightly higher on the south with a mean value of 203 K. A model of the CO (2-1) dayglow has been improved. The CO ($v = 2$) molecules are excited by absorption of the sunlight at the CO (2-0) and (3-0) bands at 2.35 and 1.58 μm and photolysis of CO_2 by the solar Lyman-alpha emission. The dayglow is quenched by CO_2, and the calculated mean dayside intensity is 3.1 MR. The weighted-mean dayglow altitude is 104 km. Variations of the dayglow with CO abundance and solar zenith angle are calculated and presented. Then the model results are used to convert the observed dayglow intensities into CO abundances at 104 km. The retrieved CO mixing ratios are constant from 50°S to 50°N with a mean value of 560 ± 100 ppm. The observed values of CO and temperatures are compared and discussed with those in other observations and models. Numerous CO and CO_2 absorption lines in the observed spectra are used to retrieve CO abundances and temperatures at 74 km on Venus. The measured CO mixing ratio is found constant at 40 ppm from 50°S to 30°N with a weak increase to the higher latitudes. The temperature at 74 km is almost constant at 222.6 ± 3.4 K, in perfect agreement with the Venus International Reference Atmosphere (Seiff, A. et al. [1985]. Adv. Space Res. 5, 3–58).

1. Introduction

Airglow is an interesting phenomenon and a tool for diagnostics of atmospheric photochemistry and dynamics. The CO dayglow at 4.7 μm was discovered on Mars (Billebaud et al., 1991) and Venus (Crovisier et al., 2006) using a high-resolution Fourier-transform spectrometer at the Canada–France–Hawaii Telescope. Those papers properly identified basic excitation processes that are absorption of the solar light by the CO (1-0), (2-0), and (3-0) bands at 4.7, 2.35, and 1.58 μm, respectively, and photolysis of CO_2. The numbers in parentheses reflect upper and lower vibrational states of the CO molecule. Crovisier et al. (2006) observed four regions of the Venus day side. Their measured intensities of the CO (2-1) and (1-0) dayglow bands were smaller than those calculated by a factor of ~2, whereas their rotational distributions resulted in weighted-mean temperatures of 189 ± 8 K at 100–110 km and 257 ± 16 K at 125–145 km, respectively.

* Address: 6100 Westchester Park Drive #911, College Park, MD 20740, USA. Fax: +1 202 319 4448.
E-mail address: vlad.krasn@verizon.net

[1] Visiting Astronomer at the Infrared Telescope Facility, which is operated by the University of Hawaii under Cooperative Agreement No. NCC 5-538 with the National Aeronautic and Space Administration, Science Mission Directorate, Planetary Astronomy Program.

http://dx.doi.org/10.1016/j.icarus.2014.04.043
0019-1035/

The CO dayglow at 4.7 μm is currently observed on both planets by the Mars Express and Venus Express orbiters using the PFS and VIRTIS-H spectrometers, respectively (Gilli et al., 2011). Sensitivities and spectral resolutions of the instruments are insufficient to detect the CO dayglow in the nadir mode. More promising is the averaging of numerous spectra in the limb observations. However, a large PFS field of view (~60 km at the best orbits) precludes any detailed study of the phenomenon. The VIRTIS-H field of view is ~5 km, and the averaged spectrum at 100 km was fitted with a reduction of the Venus International Reference Atmosphere (VIRA, Seiff et al., 1985; Keating et al., 1985) daytime temperature profile by 40 K at 90–130 km (Gilli et al., 2011). Fitting of the averaged spectrum at 150 km did not require this reduction.

Recently we observed spectra of the CO dayglow at 4.7 μm on Mars (Krasnopolsky, 2014) using the high-resolution spectrograph CSHELL at the NASA Infrared Telescope Facility (IRTF) in Hawaii. The model for the CO (2-1) dayglow excitation was significantly updated, and analysis of the observing data reveals latitudinal variations of the CO (2-1) and (1-0) dayglow, temperature and CO mixing ratio at 50 km on Mars. Here we extend the developed technique to the observation of Venus.

2. Observations

The position of NASA IRTF at the summit of Mauna Kea with an elevation of 4.2 km is advantageous for spectroscopy of planets because of the excellent astroclimate, the low atmospheric pressure of 0.6 bar, and a mean overhead water of just 2 precipitable mm. The CSHELL spectrograph (Greene et al., 1993) separates a narrow spectral interval of 0.0023 ν_0 with a central wavenumber ν_0 that may be chosen in a wide range of 1800–9000 cm^{-1} (5.6–1.1 μm, respectively). The detector is an InSb array of 256 × 150 pixels cooled to 30 K; each pixel is 9×10^{-6} ν_0 and 0.2 arcsec in the dispersion and aspect directions. The slit length is 30 arcsec, and each point of the slit results in a spectrum of 256 pixels with resolving power $\nu/\delta\nu = 4 \times 10^4$. A footprint of each spectrum is 0.2 × 0.5 $arcsec^2$, that is, 105 × 260 km^2 in our observations.

All our observations of Venus were made near maximum elongations, when the phase (Sun–Venus–Earth) angle is ~90° with the terminator just along the central meridian. Geocentric velocity of Venus is maximal at these points, providing the greatest Doppler shift. Our current observation was on August 17, 2012; Venus angular diameter was 23.0 arcsec, its geocentric velocity 13.4 km s^{-1}, and phase angle 88.4°. We placed the instrument slit parallel to the terminator near the center of the illuminated part of Venus disk. The seeing conditions were excellent, and guiding of Venus by the telescope was perfect. The overhead water was extremely low, near 0.3 pr. mm, that made it possible to observe variations of the HDO/H_2O ratio (Krasnopolsky et al., 2013); however, this is not very essential for the CO dayglow observation. Taking into account the retrograde rotation of Venus, the instrument slit covered latitudes from 60°S to 60°N at local time 07:50 near the equator, and solar zenith angle was 64° along the slit.

To observe six strongest lines of the CO (2-1) dayglow, we acquired spectra of Venus at three central wavenumbers 2137, 2144, and 2151 cm^{-1}. We also measured the sky foreground, flat field from a continuous source, and dark current for these three ranges. Absolute calibration was made using bright infrared standard stars from the IRTF catalog. However, the sky foreground is very bright at 4.7 μm, and stars of ~4th magnitude that we usually applied for calibration are not seen against this foreground. Therefore we observed Aldebaran with magnitude of −2.66 near 4.7 μm. Spectrum of a star of 0th magnitude was taken from Engelke et al. (2010). The CSHELL sensitivity is similar at three very close wavenumbers, and we observed the star only at 2144 cm^{-1}.

3. Data processing and analysis

We subtracted the sky spectra from the Venus spectra, and the results were divided by the difference between the flat field and dark current spectra. Finally, bad pixels were replaced by mean values of their two neighbors.

CO lines are rather strong in the solar spectrum and contaminate all CO lines in spectra of Mars and Venus. Heliocentric velocities of the planets are low, and both solar and planetary CO lines are almost equally Doppler-shifted. Therefore even high spectral resolution in the CFHT observations by Crovisier et al. (2006) cannot remove this contamination. Some lines of the CO dayglow are blended by Venus CO_2 lines and telluric absorption lines. Fitting by synthetic spectra is the only way to account for all these effects.

The initial phase in our technique of the fitting is conversion of the observed spectra to a wavenumber scale with a step of 0.001 cm^{-1}. We apply a parabolic fitting of three adjacent pixels to get eight sampling points per pixel and keep a sum of the sampling points at the pixel value (Krasnopolsky, 2007). (A standard parabolic fitting fixes the middle sampling point at the pixel reading.) Then a wavenumber scale is established using identified lines in a spectrum, and the spectrum is linearly interpolated to a scale with the step of 0.001 cm^{-1}. Finally three adjacent spectra are summed to further deplete the noise. A footprint of each final spectrum is 320 × 260 km^2. Spatial resolution of the combination of CSHELL and the telescope is ~1 arcsec, that is, ~500 km in our observations.

The observed and processed spectra at the equator are shown in Fig. 1. The CO (2-1) dayglow lines R4 2135.313 cm^{-1}, R5 2138.911 cm^{-1}, R6 2142.473 cm^{-1}, R7 2145.999 cm^{-1}, R8 2149.489 cm^{-1}, and R9 2152.942 cm^{-1} are remarkable at their Doppler-shifted positions. The R7 line is significantly depleted by the CO_2 line at 2146.006 cm^{-1}. The CO (2-1) dayglow lines demonstrate limb brightening that is typical of an optically thin airglow and are especially prominent at high latitudes in our geometry.

The CO (2-1) lines are not absorbed in the Venus atmosphere, because a population of CO at the first vibrational level $v = 1$ is very low. All CO absorption lines in the spectra refer to various isotopologues of the CO (1-0) fundamental absorption band. The strongest three lines are of the primary isotopologue: P2 2135.546 cm^{-1}, P1 2139.426 cm^{-1}, and R1 2150.856 cm^{-1}. They have a complicated structure and involve both telluric and Doppler-shifted venusian absorption lines. The CO (1-0) dayglow emission line is just at the center of the venusian line and greatly distorts its shape. Along with the CO (2-1) dayglow, these three lines of the CO (1-0) dayglow are the subject of our study.

The telluric CO is much less abundant than that on Venus, and other telluric CO lines are weak in the spectra. Some telluric H_2O and N_2O lines are identified in Fig. 1.

Gilli et al. (2011) calculated dayglow of the $^{13}C^{16}O$ fundamental band that appears to be weaker than that of the primary isotopologue by an order of magnitude. This dayglow is beyond our observed spectral range.

The observed spectra were adjusted for parabolic corrections to the continuum (3 parameters), sinusoidal corrections (3 parameters: amplitude, period, and phase), scattered light (1 parameter), and wavenumber corrections at the edges and in the center of each spectrum (3 parameters), that is, 10 parameters total. Synthetic spectra were calculated using abundances of CO, CO_2, and their mean temperature on Venus, abundance of telluric H_2O and its mean temperature and pressure, telluric CO, spectral resolution, solar-to-thermal emission ratio in the continuum, and dayglow line intensities. The number of the dayglow lines is four in the spectrum at 2137 cm^{-1}, two at 2144 cm^{-1}, and three at 2151 cm^{-1}; the latter includes telluric N_2O as an additional param-

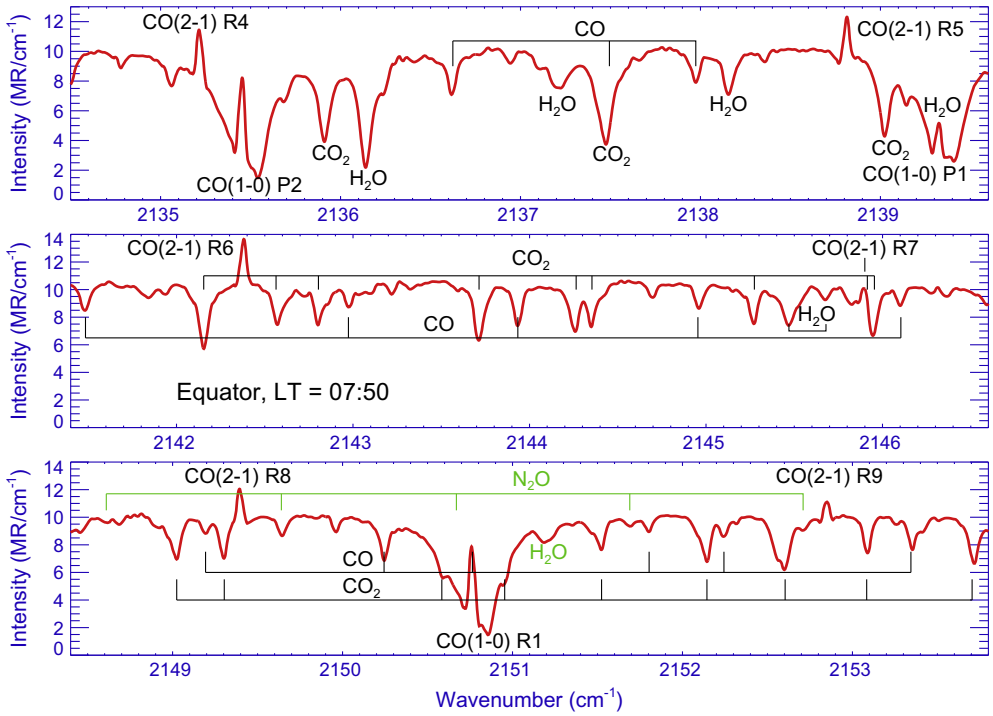

Fig. 1. Spectra of Venus observed at the equator. Six CO (2-1) and three CO (1-0) dayglow lines are identified along with absorption lines of CO and CO_2 in the Venus atmosphere and telluric H_2O and N_2O lines.

eter. The synthetic spectra also involve weak (~1%) absorption lines of telluric CO_2 and O_3 that were calculated using their fixed abundances, mean temperatures and pressures. This approach also refers to N_2O in the spectra at 2137 and 2144 cm^{-1}. Overall, the synthetic spectra involve 13 parameters (11 parameters for the spectra centered at 2144 cm^{-1}). The total number of 23 parameters is much smaller than 256 degrees of freedom (pixels) in each spectrum.

According to the Curtis–Godson approximation, absorption by a gas in an atmosphere with low aerosol extinction is equal to that of the homogeneous layer with $p = p_0/2$ and T at this level. Here p_0 is the total pressure (Chamberlain and Hunten, 1987). We apply this approximation, and our numerical test shows that its accuracy is 3–5%. This uncertainty is significantly cancelled out in the retrieved CO mixing ratios and of no interest for the telluric H_2O and N_2O.

Absorption lines of CO and CO_2 on Venus were calculated using the Voigt line shape and broadening widths of CO in CO_2 from Sung and Varanasi (2005). The retrieved CO_2 abundances give pressures for the collisional broadening. Other line parameters were taken from the HITRAN 2012 spectroscopic database (Rothman et al., 2013). The achieved accuracy of the fit is ~2.5%, lower than the one in the similar spectra of Mars because both absorption and emission lines are significantly stronger on Venus, and its spectra are more variable.

4. Results

4.1. Venus reflectivity

We use a version of the ATMOS high-resolution solar spectrum from Kurucz (2011, http://kurucz.harvard.edu/sun/atmos/). Our fitting involves comparison of the solar line depths in our spectra with those in the solar spectrum to evaluate the reflected sunlight. The absolute solar flux is equal to 10.0 erg/(cm^2 s cm^{-1}) at 1 AU in our spectral ranges (Kurucz, 2011). Assuming the Lambert reflection, properly scaled ratios of the reflected and incident solar fluxes result in Venus reflectivities shown in Fig. 2.

The retrieved reflectivities are almost constant, and some limb darkening may be partly caused by instrumental effects or deviations from the Lambert reflection at large viewing angles. The mean reflectivity is 0.077 at 2144 and 2151 cm^{-1} and smaller by a factor of 1.5 at 2137 cm^{-1}. This reduction is puzzling; however, our analysis of the observations of Venus on the next day, August 18, 2012, confirms this difference. Reflectivity of Venus is mostly determined by refractive indices of sulfuric acid. The closest points in the most detailed study of the refractive indices by Palmer and Williams (1975) are at 2120 and 2180 cm^{-1}. Broad features are typical in absorption and reflection spectra of solids and liquids, and the significant reduction from 2144 to 2137 cm^{-1} is unexpected.

Crovisier et al. (2006) observed the airglow at 4.7 μm in four regions on the Venus day side and one region on the night side. They compared the day and night side continua, applied the Galileo/NIMS observations at the same wavelength, and obtained reflectivities at four regions that varied from 0.045 to 0.12 with a mean value of 0.09 ± 0.03. Their mean value is close to those in our observations at 2144 and 2151 cm^{-1}, though we do not confirm the significant variability in the observations by Crovisier et al. (2006). Our long-slit spectrograph is better designed to study spectral variations on the planets. According to a review by Moroz (1983), spherical albedo of Venus is ~0.065 at 4 μm.

4.2. CO (1-0) dayglow

Variations of three observed lines of the CO (1-0) dayglow are shown in Fig. 3. This dayglow is excited by absorption of the sunlight by the fundamental band of CO. The absorption is very strong and optically thick; according to Crovisier et al. (2006), the dayglow originates at 125–145 km and its rotational distribution does not conform to local thermodynamic equilibrium (LTE). Crovisier et al. (2006) calculated almost equal intensities for the P2, P1

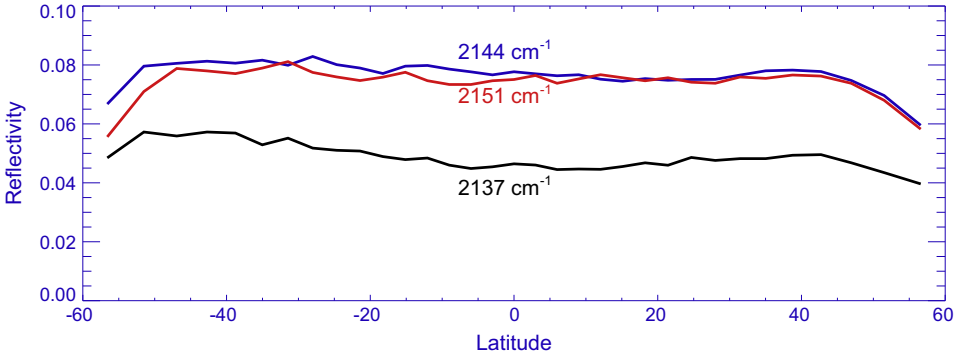

Fig. 2. Observed variations of Venus reflectivity at three wavenumbers.

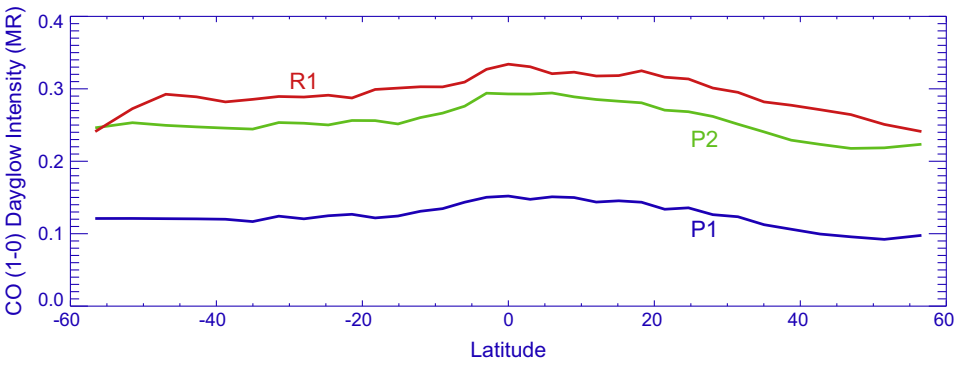

Fig. 3. Variations of the observed lines of the CO dayglow at the fundamental band (1-0).

and R1 lines, while the ratio of our observed lines in Fig. 3 is close to that of 2:1:2 for the LTE conditions. This does not prove LTE for the CO (1-0) dayglow but could indicate some problems in the calculated rotational distribution in Crovisier et al. (2006).

Mean sum of the observed P2, P1, and R1 line intensities of the CO (1-0) dayglow (Fig. 3) is 0.68 MR, and a similar value from Fig. 10 in Crovisier et al. (2006) is 0.51 MR. (One megarayleigh is an emission of 10^{12} photons per cm^2, s, and 4π sr.) The difference is small and may be caused by the larger solar zenith angles in their observations.

The CO (1-0) dayglow is optically thick, its intensity weakly depends on the CO mixing ratio in the atmosphere, and it has a non-LTE rotational distribution. Therefore this dayglow is poorly accessible for diagnostics of the atmosphere.

4.3. CO (2-1) dayglow and its latitudinal distribution

Sum of six line intensities R4–R9 is equal to a quarter of the total CO (2-1) band intensity in a broad temperature range from 130 to 250 K. This band intensity is shown in Fig. 4 and demonstrates limb brightening that is typical of an optically thin airglow. Conversion to the vertical dayglow intensity requires corrections for viewing angle ψ and reflectivity a (Krasnopolsky, 2003):

$$4\pi I = \frac{4\pi I_m}{(1/\cos\psi)_c + 2a}$$

Here the subscript c means that $1/\cos\psi$ was convolved by the instrument response function that is assumed to be a Gaussian with a full width at half maximum of 1 arcsec. The vertical intensities of the CO (2-1) dayglow are rather constant with a mean value of 3.3 MR. Its variation may be described by a standard deviation that is equal to 5%. We will discuss below the fact that vertical intensities of the CO (2-1) dayglow depend on the solar zenith angle and

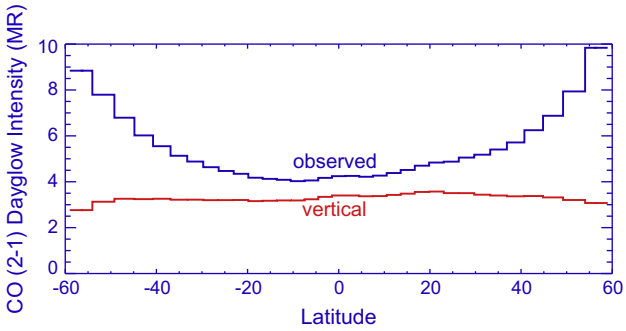

Fig. 4. Latitudinal variations of the observed and vertical intensities of the CO (2-1) dayglow.

CO abundance near 104 km. The constant vertical intensities correlate therefore with the constant solar zenith angle of 64° in our observations.

The CO (2-1) dayglow intensities and solar and viewing angles are lacking in Crovisier et al. (2006). We summed up the line intensities from their Fig. 9 and obtained a mean intensity of 4 MR. This value, once corrected for the angles and contamination by other lines, may be in reasonable agreement with our dayglow intensities.

4.4. Temperatures at 111 km

Line intensities in optically thin media are equal to their upper state populations times transition probabilities and statistical weights $2J + 1$; here J is the rotational quantum number of the upper state. According to the Boltzmann law, the population at LTE is proportional to $\exp(-\alpha E_u/T)$; here $\alpha = 1.4388$ cm K, E_u = -

$BJ(J+1)$ is the upper state rotational energy, $B = 1.89\ cm^{-1}$ is the upper state rotational constant for CO ($v = 2$). Therefore it is possible to measure atmospheric temperature using the observed line distribution. However, this requires low uncertainties of the observed line intensities. We had problems with the reflectivities extracted from the spectra at 2137 cm^{-1} and therefore do not use the R4 and R5 lines for the temperature retrieval.

The R6–R9 intensities observed at the equator and corrected for their transition probabilities and statistical weights are plotted versus rotational energy in the log scale in Fig. 5. The slope of this plot determines a temperature that is equal to 204 ± 10 K. We will show below that this temperature refers to the altitude of 111 km. Latitudinal variations of the retrieved temperature are shown in Fig. 6.

The mean retrieved temperature near 111 km (Fig. 6) is 203 K, and its variations may be described by a standard deviation of 9 K. The rotational quenching rate coefficient is $\approx 10^{-10}\ cm^3\ s^{-1}$, the number density is $7 \times 10^{13}\ cm^{-3}$ at 111 km, thus the quenching rate of 7000 s^{-1} is much larger than the CO (2-1) transition probability of 30 s^{-1}. Therefore, the rotational sublevels of the CO(2) are at LTE and the retrieved rotational temperature reflects the ambient temperature in the dayglow layer.

The Venus International Reference Atmosphere (VIRA, Keating et al., 1985) and the model by Hedin et al. (1983) give $T \approx 180$ K near 111 km based on the data from accelerometers at the Pioneer Venus and Venera probes, radio occultations at the Pioneer Venus, Magellan, and Venera 15 orbiters, and profiles of the CO_2 band at 15 μm from the Pioneer Venus and Venera 15 observations. Some of these data extend up to 100 km and were interpolated to ~145 km where the Pioneer Venus mass spectrometer and drag observations begin.

The CFHT observations of the CO (2-1) dayglow resulted in a weighted-mean temperature of 189 ± 8 K at 100–110 km (Crovisier et al., 2006). Clancy et al. (2012) derived mean dayside temperatures of $T = 186$ and 200 K at 100 km from their ground-based submillimeter observations at solar minimum and maximum, respectively. Our observations refer to mean solar activity.

High-resolution infrared heterodyne spectroscopy of the CO_2 line widths at 10.4 μm (Sonnabend et al., 2010, 2012) gives temperatures at 110 km for various conditions. The dayside temperatures vary from 200 to 240 K, and the observations at low and middle latitudes near LT = 08:00 show $T \approx 210$ K, in accord with our temperatures. A general circulation model for the Venus thermosphere (VTGCM, Brecht and Bougher, 2012) confirms this value.

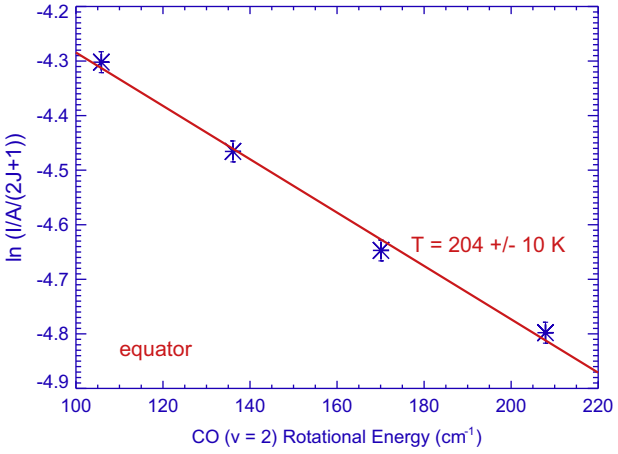

Fig. 5. Determination of rotational temperature from the observed intensities of the R6–R9 lines of the CO (2-1) dayglow. The symbol size is equal to the uncertainty of the values.

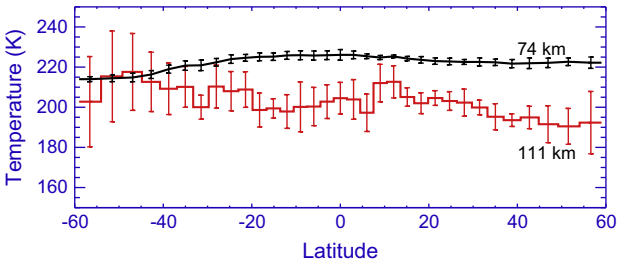

Fig. 6. Retrieved latitudinal variations of temperature at 74 and 111 km.

However, the VTGCM dayside densities near 150 km exceed those from VIRA and Hedin et al. (1983) by an order of magnitude. The densities near 150 km in the empirical models are based on the direct mass spectrometer and drag observations by the Pioneer Venus orbiter and believed to be accurate and reliable.

While the temperatures from our observations (Fig. 6) agree with those from the heterodyne spectroscopy and VTGCM, they cannot unambiguously resolve the significant difference between the empirical models and the recent version of VTGCM.

4.5. Temperature at 74 km

Venusian CO and CO_2 absorption lines are numerous and strong in our spectra. Their fits in the synthetic spectra are described by three parameters: CO and CO_2 abundances and effective temperature. Temperature determines line strengths and intensity distributions between the lines. Effective pressure is another value that is taken from the CO_2 abundance. Both reflected sunlight and thermal emission of Venus contribute to the observed spectra, and conversion of the retrieved CO_2 abundances to vertical abundances is done using the following relationship:

$$\{CO_2\} = \frac{\{CO_2\}_m}{\propto \left(\frac{1}{\cos z} + \frac{1}{\cos \psi}\right) + \frac{1-\alpha}{\cos \psi}}$$

Here $\{CO_2\}_m$ and $\{CO_2\}$ are the observed and vertical abundances, α is a share of the reflected sunlight in a spectrum, z and ψ are the solar zenith and viewing angles. Effective pressure corresponds to half vertical abundance and is corrected for 3.5% of N_2. It varies insignificantly and is equal to 15.3 ± 2.2 mbar. The relevant altitude from VIRA is 74 km.

Mean temperatures from three spectral intervals and their standard deviations are shown in Fig. 6. The observed temperature is almost constant at 222.6 ± 3.4 K. It perfectly agrees with VIRA which gives 221.0 K at 74 km for a latitude of 45°.

5. Model of the CO (2-1) dayglow

According to Billebaud et al. (1991), Crovisier et al. (2006), and Krasnopolsky (2014), the CO (2-1) dayglow is excited by photolysis of CO_2 and absorption of the sunlight by the CO (2-0) and (3-0) bands at 2.35 and 1.58 μm, respectively. The excited CO molecules either radiate the dayglow photons or are quenched by CO_2. The CO (2-1) dayglow on Earth, Venus, and Mars was calculated by Gilli et al. (2011) as a part of a sophisticated code, whose features are not discussed in detail, and the dayglow is presented in terms of vibrational temperatures that require significant conversion for comparison with observations. Here we discuss and calculate excitation and quenching of the CO (2-1) dayglow on Venus.

5.1. Model atmosphere

To model the dayglow, we need vertical profiles of T, CO_2, and CO. We adopt temperature and CO_2 profiles from VIRA for the daytime conditions at middle latitudes (Fig. 7). The CO profile is more uncertain: for example, VIRA gives a CO density at 110 km exceeding that in the model by Hedin et al. (1983) by an order of magnitude. The value from Hedin et al. (1983) at 110 km is larger than that from the photochemical model by Krasnopolsky (2012) by a factor of 1.5. However, the photochemical model is a global-mean, therefore the CO densities actually coincide at 110 km. Furthermore, the CO/CO_2 profile in Hedin et al. (1983) is in reasonable agreement with that from a recent version of VTGCM (Brecht et al., 2011). Therefore we adopt the CO profile from Krasnopolsky (2012) below 110 km and from Hedin et al. (1983) above 110 km. It is shown in Fig. 7.

5.2. Excitation processes

Using the standard assumption of the uniform excess energy distribution among degrees of freedom in the CO_2 photolysis products, Krasnopolsky (2014) argued that excitation of CO ($v = 2$) by photolysis of CO_2 is effective only for the solar Lyman-alpha emission with a yield of 0.9 (because of the excitation of $O(^1S)$ with a yield of 0.1). The Lyman-alpha intensity is 3.7×10^{11} ph cm^{-2} s^{-1} at 1 AU and mean solar activity, the CO_2 cross section is 4.5×10^{-20} cm^2 at 195 K (Yoshino et al., 1996), and the excitation rate is 330 kR for the mean dayside conditions (solar zenith angle is 60°) with a maximum at 115 km (Fig. 8).

Absorption of the solar photons by the first CO overtone (2-0) at 2.35 μm is the main excitation process. It is calculated similar to that for Mars in Krasnopolsky (2014), using 46 CO lines, 41 points in each line shape at each altitude from 70 to 150 km, collisional broadening of the CO line by CO_2 from Sung and Varanasi (2005), and the Voigt line shape. The CO (2-0) absorption lines in the solar spectrum are taken into account, though these lines are weaker than those of CO (2-1).

The CO (3-0) absorption band at 1.58 μm is weaker than the CO (2-0) band by two orders of magnitude. Almost all CO ($v = 3$) molecules cascade to $v = 2$ via radiation or collisions. The solar radiation per cm^{-1} is stronger at 1.58 μm than that at 2.35 μm by a factor of ~2, and the total number of excitations is expected to be larger by the same factor. However, the excitation occurs deeper in the atmosphere, where the CO densities as well as quenching by CO_2 are greater by two orders of magnitude. The calculated contribution of the CO (3-0) absorption band (Fig. 8) is a percent of the total CO (2-1) dayglow. Effects of CO ($v > 3$) are even smaller by orders of magnitude.

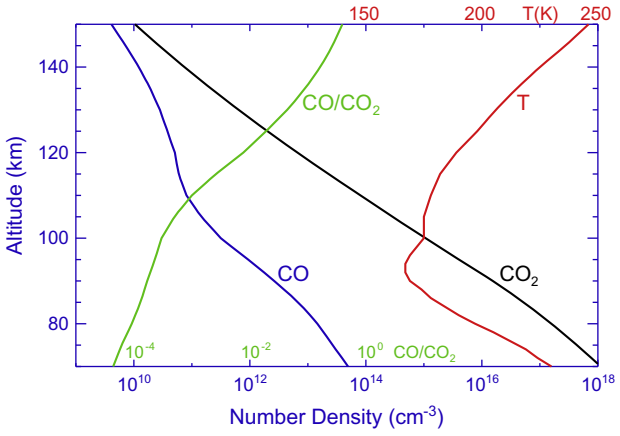

Fig. 7. Model atmosphere for calculations of the CO (2-1) dayglow.

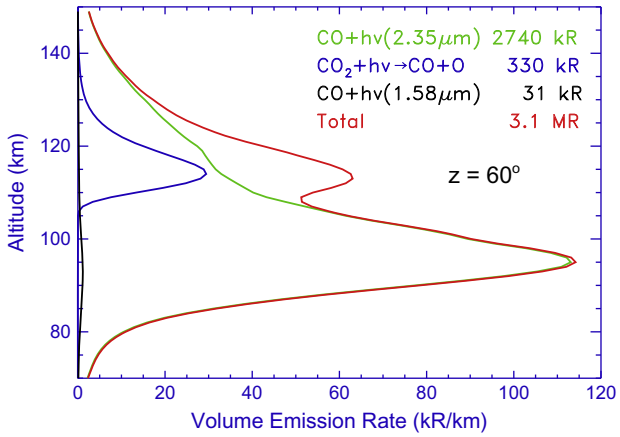

Fig. 8. Vertical profiles of volume emission rate from three processes of excitation of the CO (2-1) dayglow.

Excitation of ^{13}CO ($v = 2$) is rather similar to that of CO ($v = 3$): the ^{13}CO abundance is smaller than that of the basic isotopologue by two orders of magnitude, and the excitation occurs in the deep mesosphere, where it is strongly quenched. Furthermore, while all CO ($v = 3$) populate CO ($v = 2$), a very minor part of ^{13}CO ($v = 2$) can populate CO ($v = 2$) via exchange by two vibrational quanta with CO and by one quantum with CO ($v = 1$). The former has a low probability, and the latter is slow because of a very low density of CO ($v = 1$).

Resonant scattering of the CO (2-1) dayglow from the CO ($v = 1$) level is another excitation process. Its frequency is twice that of CO ($0 \rightarrow 1$), that is, 9.2×10^{-4} s^{-1} (Crovisier et al., 2006). Our evaluation of the CO ($v = 1$) column abundance is $\sim 10^{13}$ cm^{-2} using the CO ($v = 1$) vibrational temperature from Gilli et al. (2011). This mechanism contributes ~10 kR, i.e., 0.3% of the observed dayglow.

Excitation by

$$CO(1) + CO_2(0\,0\,1) \rightarrow CO(2) + CO_2$$

$$CO(1) + CO(1) \rightarrow CO(2) + CO$$

is generally possible; however, the reagent densities are so low that these processes may be safely neglected.

5.3. Quenching

Some reactions that are relevant to the problem are collected in Table 1. It is generally believed that the near-resonant exchange of vibrational quanta between CO, $CO_2(00v_3)$, and N_2 is much faster than vibrational-translation processes. The rate coefficients of reactions (3) and (4) confirm this hypothesis, the VT reaction (7) is slower than the VV reaction (5) by two orders of magnitude, and we will neglect the VT exchange. We will also neglect exchanges of two vibrational quanta in one collision, which is a slow process.

VV-exchange between CO(2) and CO (reaction (5)) is the only quenching of CO(2) that we have found in the literature. Its rate coefficient is 3.3×10^{-12} cm^3 s^{-1} at 200 K and exceeds that of the VV-exchange with N_2 (reaction (6)) by three orders of magnitude; the latter may be neglected.

Quenching of CO(2) by CO_2 (reaction (2)) has not been studied in the laboratory, and the closest analog is reaction (1). Rate coefficients of CO (v)–CO exchange are similar for $v = 2$ (reaction (5)) and $v = 4$ (Hancock and Smith, 1971) after correction for their endothermicities. Calculations by Jeffers and Kelley (1971) gave

Table 1
Reactions of VV and VT exchange essential for the CO (2-1) dayglow on Venus.

#	Reaction	Rate coefficient ($cm^3\ s^{-1}$)	Reference
1	$CO(1) + CO_2 \rightarrow CO + CO_2(001) - 206\ cm^{-1}$	$1.4 \times 10^{-12} \exp\left(-\frac{1119}{T} + \frac{70.900}{T^2}\right)$	Starr and Hancock (1975)[a]
2	$CO(2) + CO_2 \rightarrow CO(1) + CO_2(001) - 233\ cm^{-1}$	$1.4 \times 10^{-12} \exp(-\frac{1157}{T} + \frac{70.900}{T^2})$	See text
3	$CO_2(001) + CO \rightarrow CO(1) + CO_2 + 206\ cm^{-1}$	$1.4 \times 10^{-12} \exp\left(-\frac{829}{T} + \frac{71.600}{T^2}\right)$	Starr and Hancock (1975)[a]
4	$CO_2(001) + CO \rightarrow CO + CO_2(mn0)$	$\approx k_3/20$	Starr and Hancock (1975)
5	$CO(2) + CO \rightarrow CO(1) + CO(1) - 27\ cm^{-1}$	$5.6 \times 10^{-11} T^{-1/2} \exp(-39/T)$	Stephenson and Mosburg (1974)[b]
6	$CO(1) + N_2 \rightarrow CO + N_2(1) - 187\ cm^{-1}$	$4.3 \times 10^{-17} T \exp(-270/T)$	Stephenson and Mosburg (1974)[b]
7	$CO(1) + O \rightarrow CO + O$	2.3×10^{-14}	LVLP94[c]

Numbers in parentheses reflect vibrational levels; $v = 0$ if not shown.
[a] Our analytic approximation to the measured values.
[b] Our calculation of rate coefficients of inverse reactions to those measured.
[c] Lopez-Valverde and Lopez-Puertas (1994).

almost equal probabilities of VV-exchange for CO ($v \leqslant 4$) as well. Therefore we adopt for the quenching of CO(2) by CO_2 (reaction (2)) the rate coefficient of reaction (1) with a minor correction for the different endothermicities.

5.4. Results

Thus our model involves three excitation sources (photolysis of CO_2 by the solar Lyman-alpha and the CO absorption of the solar radiation at 2.35 and 1.58 μm), two quenching (by CO_2 and CO) processes, and spontaneous emission. The calculated vertical profiles for all components and the total dayglow are shown in Fig. 8. Actually the CO (3-0) excitation contributes 1% of the dayglow, and the quenching by CO removes 1.5% of the dayglow. Therefore our model might be further reduced to the two excitation and one quenching processes.

Using the vibrational temperatures of CO(1) from Gilli et al. (2011), we have found that the atmosphere of Venus is optically thin within the dayglow layer even in the centers of the strongest CO (2-1) lines and even at the limb, where the CO column abundances exceed the vertical CO abundances by a factor of ~50. This removes the problem of radiative transfer for the CO (2-1) dayglow.

The dayglow peaks at 96 km; however, the effective mean altitude is

$$h_0 = \frac{\int_0^\infty i(h) h dh}{\int_0^\infty i(h) dh} = 104\ \text{km}$$

The volume emission rate of the dayglow is a weighting function for two parameters that are extracted from the observed dayglow: CO abundance and temperature. The halfwidth of this function is 15 km, and the CO abundance varies significantly within 104 ± 15 km (Fig. 7). Our observational data do not account for these variations with altitude, and we adopt that the CO vertical profile from Fig. 7 is just scaled by a various factor to fit our spectra.

To obtain an effective mean altitude for our rotational temperatures, we calculate effective line strengths for the CO R6–R9 lines:

$$S_0 = \frac{\int_0^\infty i(h) S(T(h)) dh}{\int_0^\infty i(h) dh}$$

Here $T(h)$ is taken from Fig. 7 and $S(T)$ from HITRAN 2012. The calculated effective line strengths result in a rotational temperature of 179 K that corresponds to 111 km in our model (Fig. 7). Therefore the CO and T reference altitudes are 104 and 111 km, respectively.

This model was applied to calculate the CO (2-1) dayglow intensity for solar zenith angle of 64° in our observations and various CO abundances specified by a scaling factor to the CO profile in Fig. 7. The calculated dependence is shown in Fig. 9. Similarly, the dayglow vertical intensity versus cosine of solar zenith angle is shown in Fig. 10. The effective altitude varies from 107 km to 103 km with cos$z$ varying from 0.1 to 1.

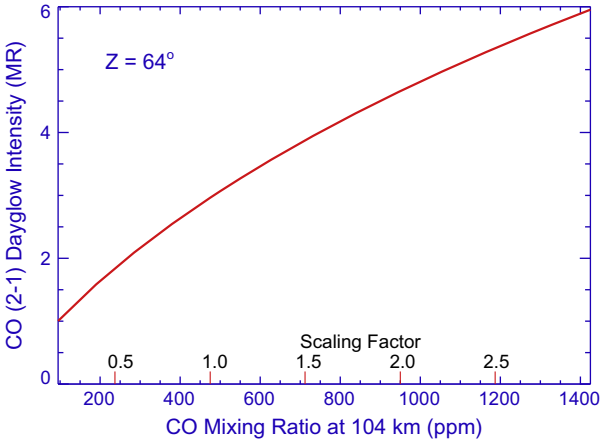

Fig. 9. CO (2-1) dayglow vertical intensity versus CO mixing ratio near 104 km at the solar zenith angle of 64°.

Using Fig. 7 from Crovisier et al. (2006), we find that their model predicts a peak CO (2-1) emission of 300 kR km^{-1} at 105 km and a vertical column emission of ~6 MR, higher than our model and observed values by a factor of 2 and exceeding their observed intensities by a factor of 2 (with proper angular corrections). The authors assumed that all CO_2 photolysis events produce CO with a flat vibrational distribution up to $v = 9$. The levels $v > 2$ cascade to $v = 2$, and an effective excitation yield of the CO (2-1) dayglow

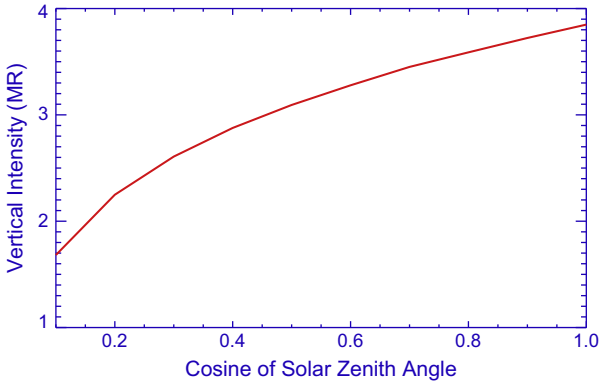

Fig. 10. CO (2-1) dayglow intensity versus cosine of solar zenith angle for the CO profile from Fig. 7.

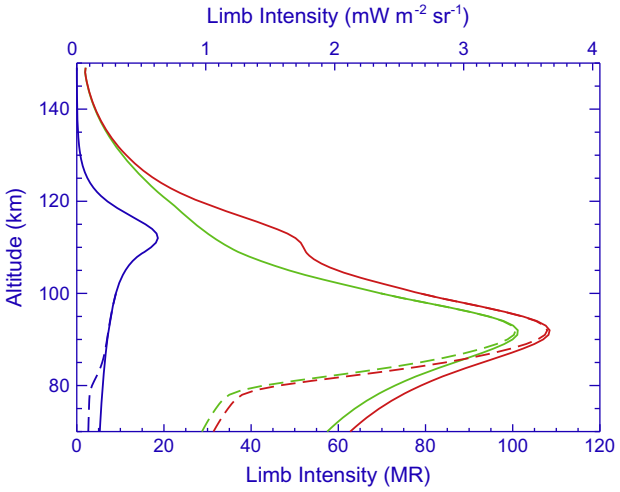

Fig. 11. Limb intensities of the CO (2-1) dayglow excitation by photolysis of CO_2 (blue), the CO (2-0) absorption (green), and total (red). Corrections for the haze absorption are shown (dashed lines). (For interpretation of the references to color in this figure legend, the reader is referred to the web version of this article.)

through photolysis of CO_2 is 0.8. The calculated (2-1) dayglow is 2 MR from photolysis of CO_2 for this assumption and exceeds that in our model by a factor of 6. The difference may be also caused by the CO profile that Crovisier et al. (2006) had taken from VIRA, which is significantly larger than that in our model. Comparison with the model by Gilli et al. (2011) requires conversions of their CO mixing ratios into CO number densities, those into the dayglow volume emission rates using the calculated vibrational temperatures and transition probabilities, and then the vertical integration; that has not been made.

Limb intensities of the CO (2-1) dayglow are shown in Fig. 11. The technique for conversion of volume emission rates into limb intensities and vise versa was developed by Krasnopolsky (1970) for optically thin airglow, and this is a case for the CO (2-1) dayglow. Absorption by the haze becomes significant below 90 km and was calculated using the particle number densities and their absorption cross sections from de Kok et al. (2011). Comparison of the calculated profile with those observed by VIRTIS at Venus Express requires separation of the CO (2-1) and (1-0) dayglow in the spectra published by Gilli et al. (2011).

6. CO mixing ratios at 104 km

The curve from Fig. 9 may be applied to convert the observed vertical intensities of the CO (2-1) dayglow (Fig. 4) into CO mixing ratios at 104 km. The results are shown in the upper panel of Fig. 12. The retrieved CO mixing ratios are rather constant in the latitude range of ±50°, and the mean CO abundance is 560 ppm at 104 km in our observations. Uncertainties of the retrieved CO abundances are mostly systematic and related to the uncertainty of the rate coefficient of quenching by CO_2 (reaction (2) in Table 1) and to the rather wide weighting function (Fig. 8) in our observations. Our tentative evaluation of the total uncertainty is 20%.

The SOIR observations of CO using three solar occultations of Venus Express gave ~200 ppm at 104 km (Vandaele et al., 2008). The observations refer to high latitude ~80°N near the terminator. Mean dayside CO abundances at 100 km are equal to 350 and 240 ppm at solar minimum and maximum, respectively, from the submillimeter observations by Clancy et al. (2012). Our results refer to mean solar activity and exceed the data by Clancy et al. (2012). However, Clancy et al. (2008) observed ~700 ppm at 104 km, close to our value. The values from the empirical models at 104 km are 400 ppm in Hedin et al. (1983) and 2200 ppm in VIRA (Keating et al., 1985). Photochemical models predict 1600 ppm (Mills and Allen, 2007), 480 ppm (Krasnopolsky, 2012), and 2300 ppm (Zhang et al., 2012). The VTGCM (Brecht et al., 2011) gives 200 ppm at noon. Therefore, there is a significant scatter in the CO mixing ratios near 104 km that covers a range of 200–2000 ppm, and our value is just in the middle of this range.

7. CO mixing ratios at 74 km

Our fitting of the observed spectra by the synthetic spectra resulted in abundances of CO and CO_2 that give CO mixing ratios after a small correction for 3.5% of N_2. Mean values from three spectral intervals and their standard deviations are shown in the lower panel of Fig. 12. The data refer to 74 km (see Section 4.5). The observed CO mixing ratio is constant at 40 ppm from 50°S to 30°N with some increase to the higher latitudes.

The observed spectra are sums of the reflected sunlight and thermal radiation of Venus. Absorption of the reflected sunlight is calculated using a simple reflection model that substitutes scattering and absorption in the real atmosphere by a simple two-way absorption by gas above a reflecting surface at some effective level. Observations of CO_2 lines may determine this level, and a ratio of

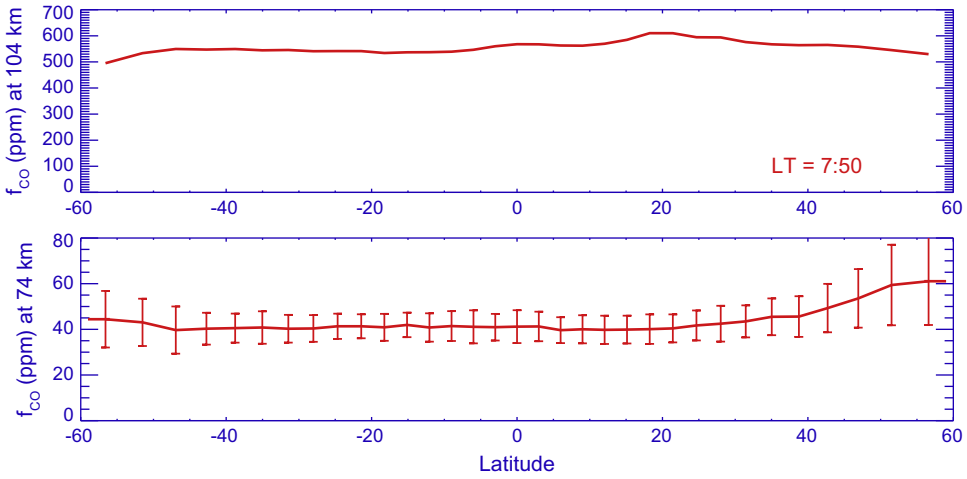

Fig. 12. Latitudinal variations of the retrieved CO abundances at 104 km and 74 km (upper and lower panels, respectively).

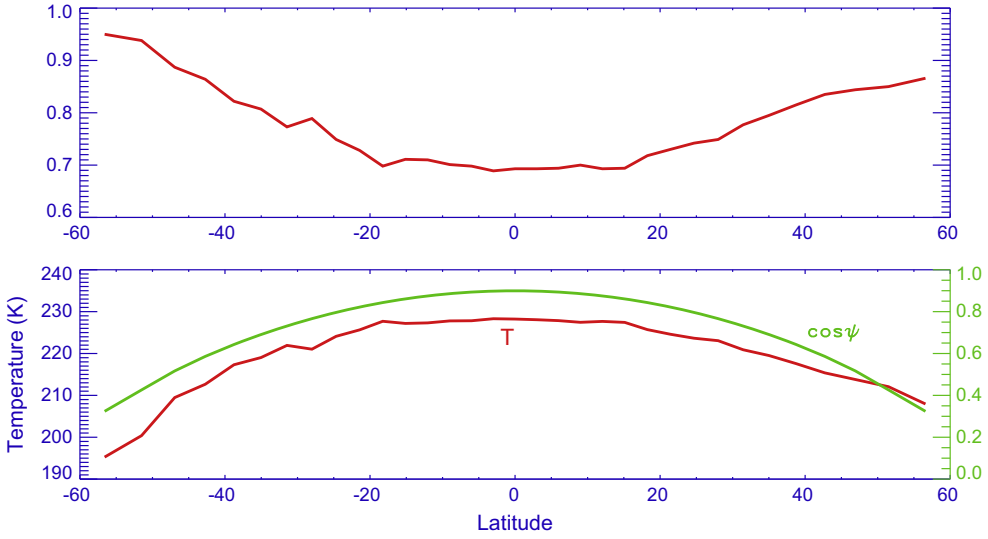

Fig. 13. Upper panel: share of the reflected sunlight in the observed spectra. Lower panel: effective temperature of Venus at 4.67 μm and cosine of viewing angle in our observations.

the observed species to the CO_2 abundance gives the species mixing ratio at a half-pressure level above the reflection level. Both absorption and thermal emission of a gas are required for analysis of thermal spectra. That has not been made in our synthetic spectra. However, thermal radiation is smaller than 30% in the observed spectra (Fig. 13, upper panel). Furthermore, the absorption is one-way and the similar approach to the CO and CO_2 lines significantly reduces errors in the CO mixing ratios.

Previous observations at 68 km give 45 ± 10 ppm (Connes et al., 1968), 51 ppm (Young, 1972), 27 ± 12 ppm (Vandaele et al., 2008), 40 ± 10 ppm (Irwin et al., 2008), and 46 ± 6 ppm (Krasnopolsky, 2010). Submillimeter observations show ~55 ppm at the lower boundary of the CO sounding at 80 km (Clancy et al., 2008, 2012). Our observations are in reasonable agreement with all these values.

The observed thermal radiation may be converted into effective temperature (Fig. 13, lower panel). It correlates with cosine of viewing angle that is typical of the atmospheres with a negative temperature gradient. The value near the vertical viewing is close to the Venus bolometric temperature of 229 ± 2 K (Schofield and Taylor, 1982).

8. Conclusions

The CO dayglow at 4.7 μm on Venus has been observed using the long-slit high-resolution spectrograph CSHELL at NASA IRTF with a resolving power of 4×10^4. The observations covered a latitude range of ±60° at a local time of 07:50 at low latitudes. Solar lines in the spectra indicate a reflectivity of 0.077 at 4.7 μm on Venus.

Three lines of the CO dayglow at the fundamental band (1-0) were measured; their intensity ratio differs from those calculated by Crovisier et al. (2006) and is closer to that expected at local thermodynamic equilibrium. The dayglow is optically thick, its intensity weakly depends on the CO abundance, and the CO (1-0) dayglow is poorly accessible for diagnostics of the Venus atmosphere.

Six observed lines of the CO dayglow at the hot (2-1) band show a significant limb brightening typical of an optically thin airglow. Vertical intensities of the CO (2-1) band corrected for viewing angle and Venus reflection are constant at 3.3 MR in the latitude range of ±50° at a solar zenith angle of 64°.

According to our estimate, the rotational temperatures of the CO (2-1) dayglow should be equal to ambient temperature near 111 km. The observed temperatures are slightly higher on the south with a mean value of 203 K, in accord with the recent infrared heterodyne observations.

A model of the CO (2-1) dayglow has been improved. The CO ($v = 2$) molecules are excited by absorption of the sunlight at the CO (2-0) and (3-0) bands at 2.35 and 1.58 μm and photolysis of CO_2 by the solar Lyman-alpha emission. The dayglow is quenched by CO_2, and its calculated mean dayside intensity is 3.1 MR. The weighted-mean dayglow altitude is 104 km. Variations of the dayglow with CO abundance and solar zenith angle are calculated and presented.

The model results are used to convert the observed dayglow intensities into CO abundances at 104 km. The retrieved CO mixing ratios are constant from 50°S to 50°N with a mean value of 560 ± 100 ppm. The observed values of CO and temperatures are compared and discussed with those in other observations and models.

Numerous CO and CO_2 absorption lines in the observed spectra are used to retrieve CO abundances and temperatures at 74 km on Venus. The measured CO mixing ratio is constant at 40 ppm from 50°S to 30°N with a weak increase to the higher latitudes. Temperature at 74 km is almost constant at 222.6 ± 3.4 K, in perfect agreement with VIRA.

Acknowledgments

This work is supported by NASA Planetary Astronomy Program (Grant NNX12AG28G to V.A. Krasnopolsky) and by Grant 11.G34.31.0074 of the Russian Government to Moscow Institute of Physics and Technology (PhysTech) and V.A. Krasnopolsky. The author is grateful to the IRTF staff and Brian Cabreira, the telescope operator.

References

Billebaud, F., Crovisier, J., Lellouch, E., Encrenaz, T., Maillard, J.P., 1991. High-resolution infrared spectrum of CO on Mars: Evidence for emission lines. Planet. Space Sci. 39, 213–218.

Brecht, A.S., Bougher, S.W., 2012. Dayside thermal structure of Venus' upper atmosphere characterized by a global model. J. Geophys. Res. 117, E08002.

Brecht, A.S., Bougher, S.W., Gérard, J.-C., Parkinson, C.D., Rafkin, S., Foster, B., 2011. Understanding the variability of nightside temperatures, NO UV and O_2 IR

nightglow emissions in the Venus upper atmosphere. J. Geophys. Res. 116, E08004.
Chamberlain, J.W., Hunten, D.M., 1987. Theory of Planetary Atmospheres. Academic, San Diego, CA.
Clancy, R.T., Sandor, B.J., Moriarty-Schieven, G.H., 2008. Venus upper atmospheric CO, temperature, and winds across the afternoon/evening terminator from June 2007 JCMT sub-millimeter line observations. Planet. Space Sci. 56, 1344–1354.
Clancy, R.T., Sandor, B.J., Moriarty-Schieven, G., 2012. Thermal structure and CO distribution for the Venus mesosphere/lower thermosphere: 2001–2009 inferior conjunction sub-millimeter CO absorption line observations. Icarus 217, 794–812.
Connes, P., Connes, J., Kaplan, L.D., Bebedict, W.S., 1968. Carbon monoxide in the Venus atmosphere. Astrophys. J. 152, 731–743.
Crovisier, J., Lellouch, E., de Bergh, C., Maillard, J.P., Lutz, B.L., Bezard, B., 2006. Carbon monoxide emissions at 4.7 μm from Venus' atmosphere. Planet. Space Sci. 54, 1398–1414.
De Kok, R., Irwin, P.G.J., Tsang, C.C.C., Piccioni, G., Drossart, P., 2011. Scattering particles in nightside limb observations of Venus' upper atmosphere by Venus Express VIRTIS. Icarus 211, 51–57.
Engelke, C.W., Price, S.D., Kraemer, K.E., 2010. Spectral irradiance calibration in the infrared. XVII. Zero-magnitude broadband flux reference for visible-to-infrared photometry. Astron. J. 140, 1919–1928.
Gilli, G. et al., 2011. Non-LTE CO limb emission at 4.7 μm in the upper atmospheres of Venus, Mars, and Earth: Observations and modeling. Planet. Space Sci. 59, 1010–1018.
Greene, T.P., Tokunaga, A.T., Toomey, D.W., Carr, J.S., 1993. CSHELL: A high spectral resolution echelle spectrograph for the IRTF. Proc. SPIE 1946, 313–323.
Hancock, G., Smith, I.W.M., 1971. Vibrational relaxation rates for CO ($v \leqslant 13$) with CO ($v = 0$), OCS, O_2 and He. Chem. Phys. Lett. 8, 41–44.
Hedin, A.E., Niemann, H.B., Kasprzak, W.T., Seiff, A., 1983. Global empirical model of the Venus thermosphere. J. Geophys. Res. 88, 73–83.
Irwin, P.G.J. et al., 2008. Spatial variability of carbon monoxide in Venus' mesosphere from Venus Express/Visible and Infrared Thermal Imaging Spectrometer measurements. J. Geophys. Res. 113, E00B01.
Jeffers, W.Q., Kelley, J.D., 1971. Calculations of V–V transfer probabilities in CO–CO collisions. J. Chem. Phys. 55, 4433–4437.
Keating, G.M. et al., 1985. Models of Venus neutral upper atmosphere: Structure and composition. Adv. Space Res. 5, 117–171.
Krasnopolsky, V.A., 1970. Nitric oxide at 110–220 km measured at the Cosmos 224 orbiter. Geomagn. Aeron. 10, 660–663.
Krasnopolsky, V.A., 2003. Mapping of Mars O_2 1.27 μm dayglow at four seasonal points. Icarus 165, 315–325.
Krasnopolsky, V.A., 2007. Long-term spectroscopic observations of Mars using IRTF/CSHELL: Mapping of O_2 dayglow, CO, and search for CH_4. Icarus 190, 93–102.
Krasnopolsky, V.A., 2010. Spatially-resolved high-resolution spectroscopy of Venus. 1. Variations of CO_2, CO, HF, and HCl at the cloud tops. Icarus 208, 539–547.
Krasnopolsky, V.A., 2012. A photochemical model for the Venus atmosphere at 47–112 km. Icarus 218, 230–246.
Krasnopolsky, V.A., 2014. Observations of the CO dayglow at 4.7 μm on Mars: Variations of temperature and CO mixing ratio at 50 km. Icarus 228, 189–196.
Krasnopolsky, V.A., Belyaev, D.A., Gordon, I.E., Li, G., Rothman, L.S., 2013. Observations of D/H ratios in H_2O, HCl, and HF on Venus and new DCl and DF line strengths. Icarus 224, 57–65.
Lopez-Valverde, M.A., Lopez-Puertas, M., 1994. A non-local thermodynamic equilibrium radiative transfer model for infrared emission in the atmosphere of Mars. 2: Daytime populations of vibrational levels. J. Geophys. Res. 99, 13117–13132.
Mills, F.P., Allen, M., 2007. A review of selected issues concerning the chemistry in Venus' middle atmosphere. Planet. Space Sci. 55, 1729–1740.
Moroz, V.I., 1983. Stellar magnitude and albedo data of Venus. In: Hunten, D.M., Colin, L., Donahue, T.M., Moroz, V.I. (Eds.), Venus. Univ. Arizona Press, pp. 27–35.
Palmer, K.F., Williams, D., 1975. Optical constants of sulfuric acid – Application to the clouds of Venus. Appl. Opt. 14, 208–219.
Rothman, L.S. et al., 2013. The HITRAN 2012 molecular spectroscopic database. J. Quant. Spectosc. Radiat. Trans. 130, 4–50.
Schofield, J.T., Taylor, F.W., 1982. Net global thermal emission from the venusian atmosphere. Icarus 52, 245–252.
Seiff, A. et al., 1985. Models of the structure of the atmosphere of Venus from the surface to 100 kilometers altitude. Adv. Space Res. 5, 3–58.
Sonnabend, G., Kroetz, P., Sornig, M., Stupar, D., 2010. Direct observations of Venus upper mesospheric temperatures from ground based spectroscopy of CO_2. Geophys. Res. Lett. 37, L11102. http://dx.doi.org/10.1029/2010GL043335.
Sonnabend, G. et al., 2012. Thermospheric/mesospheric temperatures on Venus: Results from ground-based high-resolution spectroscopy of CO_2 in 1990/1991 and comparison to results from 2009 and between other techniques. Icarus 21, 856–862.
Starr, D.F., Hancock, J.K., 1975. Vibrational energy transfer in CO_2–CO mixtures from 163 to 406 K. J. Chem. Phys. 63, 4730–4734.
Stephenson, J.C., Mosburg Jr., E.R., 1974. Vibrational energy transfer in CO from 100 to 300 K. J. Chem. Phys. 60, 3562–3566.
Sung, K., Varanasi, P., 2005. CO_2-broadened half-widths and CO_2-induced line shifts of $^{12}C^{16}O$ relevant to the atmospheric spectra of Venus and Mars. J. Quant. Spectrosc. Radiat. Trans. 91, 319–332.
Vandaele, A.C. et al., 2008. Composition of the Venus mesosphere measured by solar occultation at infrared on board Venus Express. J. Geophys. Res. 113, E00B23.
Yoshino, K., Esmond, J.R., Sun, Y., Parkinson, W.H., Ito, K., Matsui, T., 1996. Absorption cross section measurements of carbon dioxide in the wavelength region 118.7–175.5 nm and the temperature dependence. J. Quant. Spectrosc. Radiat. Trans. 55, 53–60.
Young, L.D.G., 1972. High resolution spectra of Venus: A review. Icarus 17, 632–658.
Zhang, X., Liang, M.C., Mills, F.P., Belyaev, D.A., Yung, Y.L., 2012. Sulfur chemistry in the middle atmosphere of Venus. Icarus 217, 714–739.